Robust localized-orbital transferability using the Harris functional

W. Hierse
Institut für Festkörperphysik, Technische Hochschule, D-64289 Darmstadt, Germany

E. B. Stechel
Sandia National Laboratories, MS 1421, Albuquerque, New Mexico 87185-1421

(Received 7 March 1996; revised manuscript received 30 May 96)

Replacing diagonalization in a density-functional code by an order-N algorithm does not automatically produce large efficiency gains, at least for system sizes accessible to the current generation of computers. However, both efficiency and conceptual advantages do arise from the transfer of local electronic structure between locally similar, but globally different systems. Order-N methods produce potentially transferable local electronic structure. For practical applications, it is desirable that electronic structure be transferable between subsystems of similar yet somewhat different geometry. We show, in the context of molecular deformations of a simple hydrocarbon system, that this can be accomplished by combining a transfer prescription with the Harris functional. We show proof of principle and discuss the resulting efficiency gains.
[S0163-1829(96)00647-9]

I. INTRODUCTION

It has long been recognized that there are significant advantages to the real-space description of systems containing very many atoms.[1–4] This is because chemical bonding is a local concept: Very distant regions of a large system influence each other only weakly. Kohn refers to this concept as the ''nearsightedness'' of electronic structure.[5] The advantages of designing algorithms that describe and compute the electronic structure of distant regions independently extend beyond numerical efficiency. There is also the conceptual advantage of working with quantities directly amenable to chemical interpretation.

One of the most recent attempts to exploit real-space concepts in electronic structure is the development of algorithms whose computational effort scales linearly with the number N of computed electronic states.[6–17] (N is roughly proportional to the number of atoms contained in the system.) The recognized advantage of order-N algorithms is that they can replace the conventional numerical diagonalization of a Hamiltonian matrix; the numerical effort of diagonalization is $O(N^3)$. However, this will not lead to significant increases in efficiency unless the total computational effort is dominated by the diagonalization. For instance, in density-functional theory[18,19] (DFT) algorithms using small basis sets (such as the linear combination of atomic orbitals (LCAO) method we consider here), this would be the case only for system sizes at the very limit of today's hardware capacity. For this reason, we seek additional ways of deriving computational benefits from the order-N methodology. The basic idea is to exploit the *transferability* of the local electronic structure provided by order-N algorithms.[20,11,13] Transferability is a natural consequence of the ''nearsightedness'' of electronic structure and a computational method explicitly incorporating that ''nearsightedness'' at the outset. Transferability has been explored within the Hartree-Fock formalism and other quantum-chemical approaches[21–31] as well as for chemical pseudopotentials.[29,32–35]

Whereas the majority of the quantum-chemical approaches use potentially transferable localized occupied orbitals mainly for interpretative purposes, we directly transfer localized orbitals to save numerical effort. For instance, a functional group appearing in two different molecules need not be recomputed in the second molecule if the local electronic structure can be transferred from the results of the first molecule. In this way, the effective size of the electronic structure problem can be reduced for the second molecule. The numerical advantage is of a different nature than linear scaling and does not depend on a minimal system size to become effective. We previously demonstrated[13] that in a system assembled from transferable fragments, the electronic structure can be so close to self-consistency that the self-consistent iteration became unnecessary. Explicitly, we computed the electronic structure for hydrocarbon chains of varying lengths. Once having computed the electronic structure for heptane (C_7H_{16}) with three distinct C-C bonds, terminal, one removed from terminal and internal, we had all the information needed to build the electronic structure for C_nH_{2n+2} ($n>7$) with a total-energy accuracy of fractions of an meV per chemical bond.

In the hydrocarbon results,[13] the local bond geometries remained unchanged between the systems for which the local electronic structure was transferred. However, for transferability to find widespread practical applications, it is necessary that it also be *robust* to geometric deformations. Indeed, the more robust transferability is with respect to differences in geometry, the greater the reduction in effective system size and the potential for becoming practically important.

The principal result of this paper is that it is indeed possible to gain numerical efficiency from transferability even for different geometries. However, this necessitates the development of a nontrivial transfer procedure which includes the Harris functional.[36] As an example, we consider the hydrocarbon molecule n-dodecane, shown in Fig. 1. We place special emphasis on the discussion of bond torsions, which turn out to be the deformation type most likely to result in imperfect transferability. In Sec. II, we investigate the effects of the torsion of a single bond. We find that direct orbital

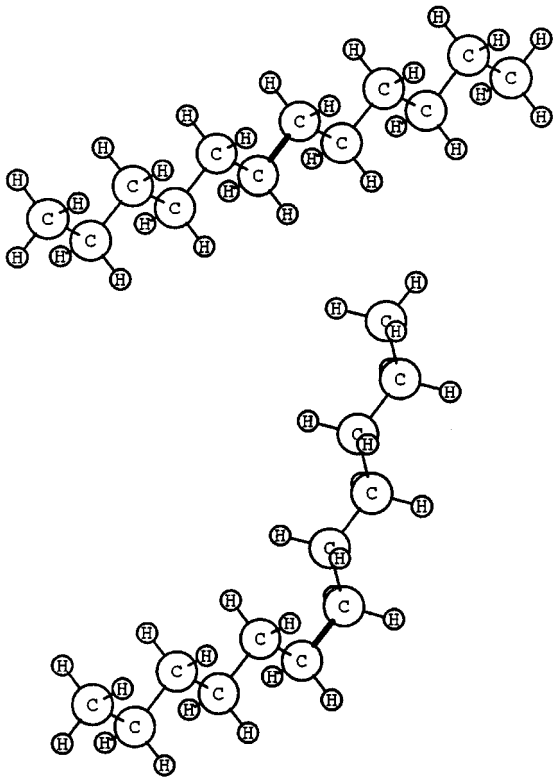

FIG. 1. The dodecane molecule in the conformations corresponding to $\alpha=0°$ (top) and $\alpha=180°$ (bottom). The bond about which the torsion is performed is denoted by a thick line.

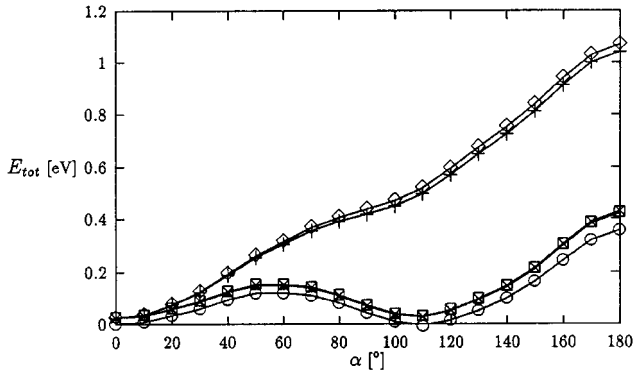

FIG. 2. Torsion barriers of the dodecane molecule (central carbon-carbon bond). ◇: Kohn-Sham functional with transferred NOLO's only. +: Transferred NOLO's, central bond self-consistently converged. ×: Transferred NOLO's, central bond and first shell of neighboring bonds self-consistently converged. □: All NOLO's self-consistently converged. ○: Self-consistent eigenstates (conventional).

transfer between the nondeformed and the deformed molecules leads to a qualitatively wrong representation of torsion barriers. In Sec. III, we overcome this limitation by combining the transfer procedure with the Harris functional. Whereas the transferred electronic structure is no longer self-consistent in the vicinity of the twisted bond, the *charge density* generated from the transferred electronic structure does produce accurate non-self-consistent Harris functional total energies. In particular, transferred orbitals produce significantly more accurate Harris functional total energies than conventionally used overlapping spherical atomic densities. Thus in circumstances of less than perfect transferability, it remains possible to use transferred electronic structure to eliminate iteration to self-consistency. Also, the diagonalization step normally required in the Harris functional can be reduced to iterative updates of only a few localized orbitals. From these results we conclude that the transferability of local electronic structure can be used to save numerical effort in realistic DFT calculations, even if the transfer is carried out between systems of locally different geometry. These efficiency gains could represent a significant impact of order-N methodology on a large range of systems. Finally, Sec. IV and Appendix A gives mathematical arguments indicating that there is not much freedom in the construction of transferable localized orbitals. Therefore, the transferability properties presented here pertain to objects reasonably well defined.

II. DIRECT LOCALIZED-ORBITAL TRANSFER

In this section, we investigate the breakdown of direct localized-orbital transfer between systems of different local geometries. As an example, we consider the linear hydrocarbon molecule n-dodecane ($C_{12}H_{26}$), shown in Fig. 1. We consider various molecular geometries (''conformations'') corresponding to the torsion angle α of the central C-C bond marked by a thick line in Fig. 1. $\alpha=0°$ is shown in the upper part, $\alpha=180°$ in the lower part of the picture. In a first step, we use a suitably adapted order-N algorithm[13] to obtain self-consistent nonorthogonal localized orbitals (NOLO's) in the conformation $\alpha=0°$. We then transfer these NOLO's to deformed geometries $\alpha\neq0°$.

The lowest curve (○) in Fig. 2 shows the torsion barriers of the dodecane molecule as obtained from conventional DFT calculations with extended eigenstates. We use the LCAO-DFT program of Feibelman[37,38] in the parallelized version, QUEST, by Sears and Schultz[39] to carry out the non-spin-polarized calculations with a minimal (''single ζ'') contracted Gaussian basis on all atoms. Hamiltonian construction scales as $O(N)$, and in combination with our order-N algorithm replacing the diagonalization (see below), the entire program scales linearly with N. Core states are eliminated by means of the pseudopotentials of Bachelet, Hamann, and Schlüter.[40] We plot the total energy as a function of the torsion angle α. The energy for $\alpha=0°$ sets the energy zero. The total-energy variations as a function of the torsion angle are only fractions of an eV. Thus, molecular torsions of the dodecane system represent a sensitive test for accuracy. The total energy shows the multiple-minima structure typical for molecular energies as a function of a bond torsion angle. The shape of this curve can be understood qualitatively in terms of steric hindrance of the functional groups rotating past each other as α increases. The structures for α and $-\alpha$ are equivalent. The calculated torsion barriers (first row of Table I) seem to agree well with typical experimental results in similar systems.[41] However, a global minimum at $\alpha\approx120°$, in contradiction to experiment, results from basis

TABLE I. Height of the dodecane torsion barriers obtained in the various calculations.

Computational method		Barrier≈60° (eV)	Barrier 180° (eV)
Conventional DFT (''exact'')		0.120	0.355
Transferred NOLO's only		(no barrier)	1.046
central bond	self-consistent	(no barrier)	1.018
optimized	Harris	(no barrier)	1.014
central bond+1st	self-consistent	0.128	0.404
NN shell optimized	Harris	0.128	0.395
all bonds	self-consistent	0.125	0.397
optimized	Harris	0.124	0.383
Harris functional	NOLO density	0.119	0.341
with eigenstates	spher. dens.	0.110	0.296

set incompleteness. An accurate determination of the torsion barriers of dodecane would involve computational details distracting from the primary focus here which is a discussion of transferability. For the sake of simplicity, we confine ourselves to an approximate computational scheme.

The second-lowest curve (□) in Fig. 2 results from self-consistent calculations using NOLO's. This set of calculations differs from the first one in that the numerical diagonalization is replaced by our order-N algorithm,[13] which describes the single-particle density operator in terms of NOLO's:

$$\hat{\rho}=2\sum_{ij}|\phi_i\rangle\mathcal{D}_{ij}\langle\phi_j|. \tag{2.1}$$

The kets $|\phi_i\rangle$ denote the NOLO's that are (approximate) linear combinations of the occupied Kohn-Sham eigenstates. At convergence, the matrix $\mathcal{D}$ approaches the inverse of the NOLO overlap matrix. We associate one NOLO with each covalent bond of the dodecane molecule. Each NOLO is expanded in terms of the atomic basis functions belonging to the two bonded atoms and the first shell of nearest-neighbor atoms. Since the localization constraints restrict the full variational freedom of the electronic structure, the curve (□) must everywhere lie above the conventional DFT results (○). The torsion barriers are given in line ''all bonds optimized—self-consistent'' in Table I. The localization-induced error in the second barrier is more than 10%. This is likely due to the rather close contact between the hydrogen atoms adjacent to the twisted bond in the $\alpha=180°$ conformation (see Fig. 1). Our NOLO localization did not allow for delocalization of the orbitals between these hydrogen atoms.

Now we turn to the curves representing total energies involving transferred NOLO's. The uppermost curve (◇) is obtained from NOLO's transferred from the linear conformation $\alpha=0°$ without further optimization. From the transferred NOLO's, we construct an input density operator $\hat{\rho}_{\rm in}$ in the form (2.1). The total energy is determined by inserting this density operator into the Kohn-Sham functional,

$$E_{\rm KS}[\hat{\rho}]=E_{\rm kin}[\hat{\rho}]+V_{\rm ext}[\hat{\rho}]+V_H[\hat{\rho}]+E_{\rm xc}[\hat{\rho}]. \tag{2.2}$$

The kinetic energy is given by

$$E_{\rm kin}[\hat{\rho}]={\rm tr}\hat{\rho}\hat{t}, \tag{2.3}$$

with the one-particle kinetic-energy operator $\hat{t}$. The external potential, Hartree, and exchange-correlation energies are functionals of the electron density

$$n(\mathbf{r})=\langle\mathbf{r}|\hat{\rho}|\mathbf{r}\rangle. \tag{2.4}$$

In transferring the NOLO's, we treat the atomic basis functions as if they are ''rigidly attached'' to the nuclei, that is, the atomic orbitals and NOLO's in the rotated half of the molecule rotate with the nuclei. For $\alpha=0°$ this transfer procedure does not change the NOLO's, and the total-energy curve (◇) obtained from transferred NOLO's must coincide with the self-consistent NOLO energy (□) at $\alpha=0°$. For increasing α, however, the transferred NOLO's close to the twisted central bond deviate increasingly from the optimized NOLO's corresponding to the $\alpha\neq0°$ geometries. One can verify this directly by comparing the corresponding orbital amplitudes. This explains the origin of the large error in the total-energy curve obtained from transferred NOLO's (◇), especially at large values of α. Indeed, nonoptimized transferred NOLO's give a qualitatively wrong description of the conformational energy.

This proves that direct NOLO transfer can fail between systems of different local geometry. Nevertheless, we describe below that transferability together with the Harris functional can be adequate. Furthermore, we note that there are still potential benefits from transferability in this example. While we essentially observed nontransferability of the NOLO's between different conformations of the dodecane molecule, this nontransferability is restricted to comparatively few NOLO's in the vicinity of the twisted bond. However, transferability still works well between the ends of the molecule because these are little affected by the bond torsion. In this way, a self-consistent DFT calculation needs to be performed only for the central part of the molecule. This represents a potentially significant reduction of the size of the self-consistent DFT problem, with corresponding savings of numerical effort. We dedicate the remainder of this section to the investigation of this possibility.

The total energies (+) in Fig. 2 are obtained from self-consistent calculations optimizing *only* the NOLO corresponding to the central bond. All the other NOLO's are constrained to match the NOLO's of the $\alpha=0°$ conformation. While in curve (+) a correction in the right direction is visible, the conformational energy retains its qualitatively wrong shape displaying only one torsion barrier. This

changes dramatically if in addition to the central bond the shell of nearest-neighbor C-C and C-H bonds are variationally and self-consistently optimized (×). We obtain torsion barriers of 0.128 and 0.404 eV (''central bond + 1st NN shell optimized–self-consistent'' in Table I, as compared with 0.125 and 0.397 eV for the self-consistent treatment of all NOLO's (''all bonds optimized—self-consistent''). As compared with curve (◇) (optimization of only the central bond), this represents a reduction in error by a factor of 50.

In summary, self-consistent iteration of only seven of the 37 NOLO's representing the molecular electronic structure recovers the torsion barriers to an accuracy of 7 meV or 2%. Thus, local iteration of a region independent of the total size of the system is sufficient to obtain correct torsion barriers, while the remainder of the system's electronic structure can be transferred from the $\alpha=0°$ conformation. In conclusion, for this example transferability has significantly reduced the size of the effective DFT problem. Extended eigenstates would have 2738 variational parameters. The formulation in terms of NOLO's has already reduced the scale of the problem to 560 variational parameters. The seven optimized orbitals have only 116 variational parameters. This corresponds to 21% of the NOLO parameter space and only 4% of the parameter space of delocalized eigenstates.

III. COMBINATION OF ORBITAL TRANSFER AND HARRIS FUNCTIONAL

In this section, we describe how NOLO transferability enables the accurate non-self-consistent calculation of torsion barriers by means of the Harris functional. The Harris functional is a method for obtaining non-self-consistent approximations of the total energy from a guess for the electron density. The deviation from the true, self-consistent energy is of second order in the error in the guessed electron density. Here, we obtain the input electron-density operator $\hat{\rho}_{\rm in}$ from transferred NOLO's, using (2.1). The Harris functional $E_H[\hat{\rho}_{\rm in}]$ is related to the Kohn-Sham functional (2.2) through

$$E_H[\hat{\rho}_{\rm in}]=E_{\rm KS}[\hat{\rho}_{\rm in}]+{\rm tr}(\hat{\rho}_{\rm out}-\hat{\rho}_{\rm in})\hat{H}_{\rm KS}[\hat{\rho}_{\rm in}]. \qquad (3.1)$$

The various quantities appearing in (3.1) are defined as follows: $\hat{H}_{\rm KS}[\hat{\rho}_{\rm in}]$ is the Kohn-Sham Hamilton operator defined as the functional derivative of the Kohn-Sham functional with respect to the density operator

$$\hat{H}_{\rm KS}[\hat{\rho}]=\delta E_{\rm KS}[\hat{\rho}]/\delta\hat{\rho} \qquad (3.2)$$

and evaluated at the non-self-consistent density $\hat{\rho}=\hat{\rho}_{\rm in}$. $\hat{\rho}_{\rm out}$ is the ground-state density operator of the (in general, non-self-consistent) Hamiltonian $\hat{H}_{\rm KS}[\hat{\rho}_{\rm in}]$, i.e., the output of the first self-consistent iteration. Conventionally, $\hat{\rho}_{\rm out}$ is obtained by finding the N lowest eigenstates of $\hat{H}_{\rm KS}[\hat{\rho}_{\rm in}]$.

Here, our linearly scaling NOLO algorithm[13] replaces the numerical diagonalization to obtain $\hat{\rho}_{\rm out}$ from $\hat{H}_{\rm KS}[\hat{\rho}_{\rm in}]$. As in Sec. II, we consider the optimization of the central bond only, an optimization of the central bond plus the first shell of neighboring bonds, and an optimization of all the NOLO's in the system. The resulting Harris functional curves are extremely close to the corresponding energies obtained from local self-consistent iteration [(+), (×), and (□) in Fig. 2]: The resulting diagram looks almost identical to Fig. 2. It is more informative to note the absolute magnitude of the torsion barriers; we give these in Table I. The torsion barriers obtained from local self-consistent iteration and the corresponding Harris functional deviate by no more than a few meV. By contrast, the inaccuracy of the torsion barriers due to the use of NOLO's instead of eigenstates is of the order of a few meV for the first barrier and of a few tens of meV for the second one. Indeed, the inaccuracy due to the non-self-consistent treatment is negligible in comparison with the error introduced by the NOLO description itself. We conclude that for this case of imperfect transferability, the self-consistent iteration can be eliminated, just as in the hydrocarbon results of Ref. 13. The non-self-consistent Harris functional, evaluated with transferred NOLO's, achieves the same overall accuracy as the local self-consistent iteration, but at significantly lower cost.

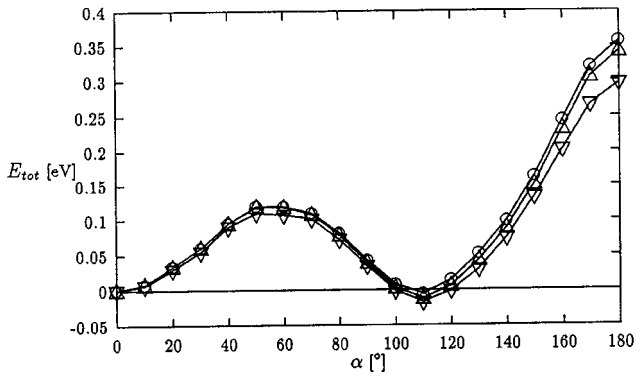

FIG. 3. Torsion barriers of the dodecane molecule (central carbon-carbon bond), comparison of input densities for the Harris functional. ○: Self-consistent eigenstates (conventional). △: Harris functional with numerical diagonalization, input density from transferred NOLO's. ▽: Harris functional with numerical diagonalization, input density from overlapping spherical atomic densities.

Frequently, the Harris functional is applied in conjunction with input electron densities constructed from overlapping spherical atomic densities.[36,42–44] It is of interest to compare the quality of our input density constructed from NOLO's with an input density obtained in this more traditional way. We carry out two sets of Harris functional calculations, using numerical diagonalization to obtain $\hat{\rho}_{\rm out}$ in each case. The first set of calculations, leading to total-energy curve (△) in Fig. 3, is done with input charge densities obtained from transferred NOLO's, the second one (▽) with overlapping atomic densities. In the construction of the spherical densities we assign occupations of one electron to the s shell and three electrons to the p shell of the C atoms, corresponding to the sp^3 hybridization state. Manifestly, the Harris functional obtained from the NOLO-generated electron density (△) represents the self-consistent energies (○) better than the Harris functional obtained from overlapping spherical atomic densities (▽). Also, we point out that the energy origin of the curves (○) and (△) is the same, whereas the curve (▽) has been shifted up by almost 2 eV to fit into the diagram. In other words, the error in the total energy for overlapping atomic spheres is of the order of 2 eV. The resulting torsion barriers are given at the bottom of Table I. The resulting errors in the first and second barrier from using the transferred NOLO densities and the Harris functional are 1 and 14

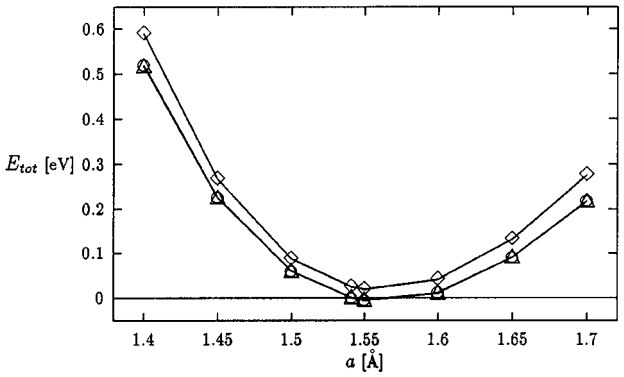

FIG. 4. Stretching of the central carbon-carbon bond in dodecane. ◇: Kohn-Sham functional with transferred NOLO's only. △: Harris functional with numerical diagonalization, input density from transferred NOLO's. ○: Self-consistent eigenstates (conventional).

meV, respectively. This compares to 10 and 59 meV for the Harris functional with overlapping spherical densities. We conclude that the NOLO density approximates the self-consistent electron density significantly better than the overlapping atomic densities. We did not attempt to systematically optimize the atomic densities to obtain better agreement with the self-consistent density, and a better quality of the atomic densities may be achievable.[42,43,45,46] As we are considering a situation of covalent bonding, the difference in accuracy should at least, in part, result from the bond charges that are present in the NOLO density, but not in *any* superposition of spherical densities.[47] The implication is that transferable NOLO's can represent a mechanism to obtain accurate input electron densities to be used in the Harris functional. We point out, however, that the evaluation of the Harris functional with NOLO's requires a solution of the Poisson equation that can be avoided when the input charge density is obtained from overlapping fragment densities whose electrostatic potentials are known from the outset.[36] Nevertheless, the electrostatic potential can be separated into two terms, one arising from the overlapping atomic sheres and one from the remainder. The potential from the remainder can be determined by a fast Fourier transform on a coarse grid.[38]

In order to get a more complete idea of how accurately the entire molecular total-energy surface is represented by NOLO transfer plus Harris functional, we briefly consider deformations other than bond torsions. In Fig. 4, we show the total energy as a function of the length of the central bond in dodecane. From the self-consistent treatment using eigenstates (○) we obtain an equilibrium length of ca. 1.55 Å, as compared with the experimental value of 1.54 Å.[48] This good agreement should be viewed with caution as we are dealing with minimal basis sets and converged calculations should have bond lengths slightly shorter than experiment. A quadratic fit to this curve results in a force constant of 33.2 eV/Å^2. (The experimental value is 28.1 eV/Å^2.[49]) Direct evaluation of the Kohn-Sham functional with transferred NOLO's, using the transfer prescription of Sec. II, gives the curve (◇). It is almost uniformly shifted with respect to the self-consistent curve and has a force constant of 36.8 eV/Å^2, which is 10% larger than the self-consistent

TABLE II. Total-energy increase of the dodecane molecule at random perturbation of the ground-state geometry.

	ΔE_{tot} (meV/orbital)		
$\sqrt{\langle r^2 \rangle}$ (Å)	Conventional DFT (''exact'')	Transferred NOLO's only	Harris functional with eigenstates—NOLO density
0.0025	0.491	0.524	0.490
0.0050	1.617	1.755	1.613
0.0075	3.381	3.694	3.371
0.0100	5.790	6.348	5.771
0.0125	8.844	9.720	8.815
0.0150	12.546	13.814	12.506

value. We note that in contrast to the bond torsions considered above, the total-energy variations associated with changes of bond lengths are *qualitatively correctly* described by a straightforward NOLO transfer without any further optimizations. The corresponding force constants, however, are too large. This is because the NOLO's used here minimize the total energy for the equilibrium geometry. In modified structures, the transferred NOLO's are no longer optimal, leading to increased total energies and a consequent apparent ''stiffening'' of the geometry. In Fig. 4, we also give Harris functional values obtained from the NOLO input density (△) and numerical diagonalization of the corresponding Hamiltonian [see Eq. (3.1)]. This curve almost perfectly matches the self-consistent energies (○). The corresponding force constant is 33.0 eV/Å^2. It is smaller than the self-consistent value because the Harris functional obeys a *maximum principle*, i.e., the nonoptimal NOLO's in the nonequilibrium geometries give total energies that are too small, causing an apparent ''softening'' of the molecule with a force constant that is too small by only 1%, as compared to the self-consistent value.

We obtain analogous results for random perturbations of the molecular equilibrium structure. We modify each nuclear coordinate by Gaussian-distributed random numbers in such a way that the average of the three-dimensional displacement length $\sqrt{\langle r^2 \rangle}$ has a given value. The RMS displacements chosen and the resulting increases of the self-consistent total energy per NOLO are given in the first two columns of Table II. For the maximal RMS displacement of 0.015 Å the total energy increase roughly corresponds to the thermal average of potential energy at room temperature. Evaluation of the Kohn-Sham functional with transferred NOLO's (third column) gives total-energy differences that are consistently about 10% too large. This roughly corresponds to the increase in the force constant of the central bond described above. The Harris functional, evaluated with the NOLO density, again represents the total-energy differences quite faithfully, with errors of less than half a percent.

In summary, the combination of NOLO transfer and the Harris functional enables the elimination of the self-consistent iteration even in situations where direct NOLO transfer is not sufficiently accurate. Among all types of molecular deformations considered, bond torsion turns out to be most problematic with respect to transferability. However, even in this case the Harris functional yields reasonably ac-

curate torsion barriers. Furthermore, the evaluation of the Harris functional with transferred NOLO's proves significantly more accurate than starting from overlapping spherical atomic charge densities.

IV. UNIQUENESS PROPERTIES OF TRANSFERABLE LOCALIZED ORBITALS

All of the preceding results and discussion were based on a particular choice for orbital localization. We chose bond-centered orbitals. However, there are different possibilities for localizing orbitals within the DFT formalism. Therefore, it is necessary to address the question: In what way do the results of this work depend on the particular choice of orbital localization?

Order-*N* algorithms have been successfully applied with bond-centered,[10,11,13] interstitial centered,[11] atom-centered,[9] and ''floating'' orbitals confined to certain regions of space, but independent of the atom positions.[7] In all these applications, however, the focus was on linear scaling, not on transferability. We argue that, if an order-*N* method is specifically adapted for the purpose of transferability (as in our case), then not all localization prescriptions are equivalent. Since for a given problem the localized orbitals strongly depend on the localization constraints, the localized orbitals can be optimally transferable only if the localization prescription itself is transferable. This means that the same localization prescription must not only be applicable to the different systems between which we wish to transfer the orbitals, but it must also lead to similarly and physically reasonable localized orbitals in each case. To illustrate how stringent this requirement is in practice, we briefly demonstrate why atom centering (the only other reasonable candidate) cannot furnish physically reasonable transferable orbitals even within the class of saturated hydrocarbon molecules.

We assume that we wish to treat the stretched polyethylene chain (the infinite analog of the linear dodecane molecule) with atom-centered localized orbitals. For maximal transferability of these orbitals, it is certainly necessary that the orbital arrangement have the periodicity of the molecule. (In closed-shell systems, the ground state always transforms according to the identical representation of the molecular symmetry group. A periodic arrangement of orbitals is thus consistent with the symmetry of the ground state.) We can therefore restrict our attention to the CH_2 monomer. The CH_2 unit contains six valence electrons, corresponding to three doubly occupied localized orbitals. Assume that from a localized-orbital computation we obtained these three self-consistent orbitals, which we now want to transfer to a finite hydrocarbon, such as the dodecane molecule. No problem occurs with the transfer to the internal CH_2 units of the dodecane. The terminal CH_3 groups, of course, were not contained in the polyethylene and need to be computed separately. However, now we have a problem with orbital localization within the terminal CH_3 groups: Each contains seven valence electrons. Therefore, there must be at least one singly occupied orbital in each CH_3 group, and the molecular electronic structure corresponds to a di-radical, not the molecular ground state.

In a very large class of systems, similar arguments show unambiguously what the physically relevant localization prescription should be. In metals it is less obvious.[11] In some closed-shell cases, it will not be obvious and some experimentation will become necessary. In open-shell systems, in general, one will likely have to deal with fractionally occupied localized orbitals about whose transferability properties we cannot draw any conclusions from the results on hydrocarbons. For the hydrocarbons, we suspect that bond centering is the only reasonable possibility, although we are not aware of any rigorous proof.

In this paper we have presented results using a minimal basis set. We should note that the dependence of accuracy versus localization radius appears to be significantly basis-set dependent. Preliminary results on hydrocarbons with a double-ζ basis indicate that the total-energy inaccuracy introduced by our localization scheme is approximately 10 times larger (although still small) than the single-ζ calculation. This needs further investigation.

Last, we address the question of uniqueness within a given localization constraint. This is just as important for practical applications of transferability. For example, if for a given system a self-consistent NOLO calculation could converge to two different sets of NOLO's (e.g., depending on start values) representing the same ground state, then orbitals taken from these two sets could not necessarily be combined to reconstruct a consistent electronic structure. It would then be even more uncertain if transferability between *different* systems could work, e.g., in the sense of ''patching together'' an approximate molecular electronic structure from parts of systems computed previously.

In Appendix A, we present a mathematical argument that such a problem will generally not arise. We show that, in general, the solution of converged NOLO's is unique up to a mixing of NOLO's literally within the same localization region. Since, in the alkanes, all NOLO localization regions are distinct, we may safely assume that the solution found is unique. We confirmed this to ourselves by running a model tight-binding calculation on a linear chain. We started from random numbers within the localization region. While it took a long time to converge, the final solution was always independent of the starting point.

We conclude that the choice of localization regions is strongly restricted by the requirement of transferability, and that the NOLO's are, in general, uniquely determined within a given localization prescription. This may be an unexpected result in light of the large arbitrariness that exists in forming nonorthogonal linear combinations from the occupied Kohn-Sham states. At least for covalent, closed-shell systems, the concept of an optimally transferable, nonorthogonal localized orbital appears to be reasonably well-defined, although the mathematical arguments presented are not at the level of a rigorous proof. Nevertheless, this increases the potential relevance of the empirically observed transferability properties that we investigated herein.

V. CONCLUSION

The results presented indicate that nonorthogonal localized-orbital transferability enables a reliable partially self-consistent or non-self-consistent representation for the total-energy surface of the dodecane molecule. Compared to a conventional self-consistent approach, twofold savings are

realized: First, by reducing the effective system size of the variational and self-consistent treatment and second, by replacing the self-consistent iteration with the Harris functional. Our main conclusion is that transferability of nonorthogonal orbitals can be robust enough to be applicable even between different system geometries.

We found that in some cases (such as bond stretching and random perturbations of molecular geometry), straightforward localized orbital transfer is sufficient to give an accurate non-self-consistent total-energy surface. For other types of deformations, such as bond torsions, such a procedure is not accurate enough to give qualitatively correct total energies. Nevertheless, in the latter case, the transferred NOLO's produce a screening potential resulting in highly accurate Harris functional total energies even for extreme deformations. There is reason to believe that Harris functional input densities generated from transferred NOLO's should frequently be superior in quality to input densities obtained as superpositions of spherical atomic densities.

While our work focused on NOLO transferability in the context of Gaussian-based LCAO-DFT, the basic concept is independent of the representation. In particular, it should be possible to apply transferability with conjugate-gradient DFT algorithms representing localized wave functions on a real-space grid. We believe that a critical ingredient to the practicality of the method is that localized orbitals are allowed to be nonorthogonal. Within a formalism relying on orbital orthogonality, transferability would not result in accurate electronic structure because orthogonality is, in general, lost when localized orbitals are transferred to a different system. Also, orthogonal orbitals are necessarily less localized than NOLO's for the same level of accuracy, resulting in less flexible transferability.

More general conclusions about the attainability of robust transferability within DFT could be drawn as soon as the performance of electronic structure transferability has been analyzed in a broader context. In addition to the transferability of electronic structure between different geometries of the same chemical system, transferability between chemically different environments should be investigated. Another important aspect would be the applicability of transferability in systems with a certain degree of delocalization in the electron system. The results presented here encourage a full exploration of electronic structure transferability as a qualitatively different way to increase numerical efficiency utilizing order-N methods.

ACKNOWLEDGMENT

The calculations were performed at the Massively Parallel Computing Research Laboratory at Sandia National Laboratories, New Mexico, whose assistance is gratefully acknowledged. W.H. thanks Dr. J. Kübler, Dr. M. P. Sears, and Dr. P. A. Schultz for helpful discussions. This work was supported by the United States Department of Energy under Contract No. DE-AC04-94AL85000.

APPENDIX A: UNIQUENESS OF NOLO'S AT GIVEN LOCALIZATION CONSTRAINTS

In this appendix we prove that the localized orbitals are unique within a given (finite) localization constraint. The functional from which the localized orbitals are obtained at a fixed Hamiltonian (cf. Ref. 13) can be written in the form

$$F = 2\,\mathrm{tr}(2 - DS)DH. \tag{A1}$$

D, S, and H are $M \times M$ matrices, M being the dimension of the LCAO basis set. S is the overlap matrix of the LCAO basis, and H is the Hamiltonian matrix minus a suitable multiple of the overlap. D is defined by

$$D = c\mathcal{D}c^{\dagger}, \tag{A2}$$

where c is an $M \times N$ matrix containing the LCAO expansion coefficients of the NOLO's and $\mathcal{D}$ is a general symmetric $N \times N$ matrix. Note that D converges to the density matrix in the LCAO representation. The functional F is then minimized independently with respect to c and $\mathcal{D}$. For unconstrained minimization and closed-shell systems, F can be shown to have a unique minimum with respect to D. The D minimizing F is equal to the LCAO projection of half the ground-state density operator of H. During the minimization, orbital localization can be enforced by allowing only certain elements of the c matrix to be nonzero. In the presence of not too strong NOLO localization, the minimum of F will still be close to the ground-state density operator, and unique. At convergence, the c matrix contains the LCAO components of the optimized NOLO's $|\phi_i\rangle$,

$$|\phi_i\rangle = \sum_{\alpha=1}^{M} c_{\alpha i}|\alpha\rangle. \tag{A3}$$

$|\alpha\rangle$ being the αth LCAO basis function. The matrix $\mathcal{D}$ converges to the inverse of the NOLO overlap matrix appearing in Eq. (2.1). However, it is not yet clear that not only the converged D, but also c and $\mathcal{D}$ separately are unique. Indeed, a linear transformation

$$c \mapsto c' = c\mathcal{A}, \tag{A4}$$

$$\mathcal{D} \mapsto \mathcal{D}' = \mathcal{A}^{-1}\mathcal{D}(\mathcal{A}^{-1})^{\dagger}, \tag{A5}$$

with an arbitrary, nonsingular $N \times N$ matrix $\mathcal{A}$ would leave D invariant. We have to show that any transformation $\mathcal{A}$ not violating the localization constraints is trivial (such as a multiplication of each NOLO with a factor).

We define the ''localization'' z_i of NOLO $|\phi_i\rangle$ (represented by the ith column of c) as the subset of LCAO basis function indices α for which $c_{\alpha i}$ is allowed to be nonzero. For each NOLO the number of such α indices is independent of the system size and thus $O(1)$. If $z_j \subseteq z_i$, then $|\phi_j\rangle$ fulfills localization z_i, but $|\phi_i\rangle$ does not necessarily fulfill localization z_j. For what follows, it is useful to abbreviate the ith column of c by $\mathbf{c}_i$. $\mathbf{c}_i$ is the vector of LCAO coefficients defining NOLO $|\phi_i\rangle$. With this notation, we write (A4):

$$\mathbf{c}_i' = \sum_j \mathcal{A}_{ji}\mathbf{c}_j. \tag{A6}$$

We define a vector $\mathbf{f}_i$ by

$$\mathbf{f}_i \equiv \mathbf{c}_i' - \sum_{z_j \subseteq z_i} \mathcal{A}_{ji}\mathbf{c}_j = \sum_{z_j \not\subseteq z_i} \mathcal{A}_{ji}\mathbf{c}_j. \tag{A7}$$

The sum over j with $z_j \subseteq z_i$ runs over $O(1)$ indices, whereas the sum with $z_j \not\subseteq z_i$ runs over $O(N)$ indices. If we require $\mathbf{c}_i'$ to fulfill localization z_i, the same is true for $\mathbf{f}_i$. To find a

nontrivial transformation $\mathcal{A}$ from $\{\mathbf{c}_i\}$ to $\{\mathbf{c}_i'\}$, we must determine coefficients $\mathcal{A}_{ji}$ in such a way that $\mathbf{f}_i \neq 0$.

Equation (A7) expresses equality of two vectors in the M-dimensional space of LCAO coefficients. Since $\mathbf{f}_i$ is subject to localization z_i, the left-hand side is restricted within a $O(1)$-dimensional subspace U_1. The right-hand side is a general vector in a subspace U_2 spanned by the vectors $\{\mathbf{c}_j, z_j \not\subseteq z_i\}$. The dimension of U_2 is $O(N)$, yet for any realistic LCAO basis we have $M - \dim U_2 = O(N) > 0$. Especially the inequality $\dim U_1 + \dim U_2 < M$ is always fulfilled. Now, what is the dimension of the subspace of vectors solving (A7), that is, $\dim(U_1 \cap U_2)$?

From linear algebra, we have

$$\dim(U_1 \cap U_2) = \dim U_1 + \dim U_2 - \dim(U_1 + U_2) \quad \text{(A8)}$$

($U_1 + U_2$ is the subspace of linear combinations of U_1 and U_2.) To determine $\dim(U_1 + U_2)$, we note that the ''orientations'' of U_1 and U_2 in M-dimensional space are ''uncorrelated'' in the following sense: U_1 is determined solely by the manually assigned localization z_i, whereas U_2 is determined by the ground-state density operator, i.e., by the physically determined quantities H, S, and the particle number of $2N$. For ''uncorrelated'' subspaces with a combined dimension less or equal the dimension of the embedding space, we, in general, have (except in the unlikely case of accidental alignment)

$$\dim(U_1 + U_2) = \dim U_1 + \dim U_2 . \quad \text{(A9)}$$

In the sense of a probabilistic statement, the dimensions of uncorrelated subspaces are additive. Combining (A8) and (A9), we obtain $\dim(U_1 \cap U_2) = 0$, which only permits the trivial solution $\mathbf{f}_i = 0$ and $\mathcal{A}_{ji} = 0$, $z_j \not\subseteq z_i$ to (A7). This is equivalent to

$$\mathbf{c}_i' = \sum_{z_j \subseteq z_i} \mathcal{A}_{ji} \mathbf{c}_j , \quad \text{(A10)}$$

hence $\mathbf{c}_i'$ is a linear combination of the at most $O(1)$ NOLO's, whose localizations are completely contained in z_i.

[1] V. Heine, in *Solid State Physics: Advances in Research and Applications*, edited by H. Ehrenreich, F. Seitz, and D. Turnbull (Academic, New York, 1980), Vol. 35.
[2] F. García-Moliner and J. Rubio, J. Phys. C **2**, 1789 (1969).
[3] F. García-Moliner and J. Rubio, Proc. R. Soc. London, Ser. A **324**, 257 (1971).
[4] J. E. Inglesfield, J. Phys. C **4**, L14 (1971).
[5] W. Kohn, Phys. Rev. Lett. **76**, 3168 (1996).
[6] W. Yang, Phys. Rev. Lett. **66**, 1438 (1991).
[7] G. Galli and M. Parrinello, Phys. Rev. Lett. **69**, 3547 (1992).
[8] X.-P. Li, R. W. Nunes, and D. Vanderbilt, Phys. Rev. B **47**, 10 891 (1993).
[9] F. Mauri, G. Galli, and R. Car, Phys. Rev. B **47**, 9973 (1993).
[10] P. Ordejón, D. A. Drabold, M. P. Grumbach, and R. M. Martin, Phys. Rev. B **48**, 14 646 (1993).
[11] E. B. Stechel, A. R. Williams, and P. J. Feibelman, Phys. Rev. B **49**, 10 088 (1994).
[12] F. Mauri and G. Galli, Phys. Rev. B **50**, 4316 (1994).
[13] W. Hierse and E. B. Stechel, Phys. Rev. B **50**, 17 811 (1994).
[14] A. Alavi, J. Kohanoff, M. Parrinello, and D. Frenkel, Phys. Rev. Lett. **73**, 2599 (1994).
[15] E. Hernández and M. J. Gillan, Phys. Rev. B **51**, 10 157 (1995).
[16] S. Goedecker, J. Comput. Phys. **118**, 261 (1995).
[17] Y. Wang, G. M. Stocks, W. A. Shelton, and D. M. C. Nichelson, Phys. Rev. Lett. **75**, 2867 (1995).
[18] P. Hohenberg and W. Kohn, Phys. Rev. **136**, B864 (1964).
[19] W. Kohn and L. Sham, Phys. Rev. **140**, A1133 (1965).
[20] W. Kohn, Chem. Phys. Lett. **208**, 167 (1993).
[21] S. F. Boys, Rev. Mod. Phys. **32**, 296 (1960).
[22] S. Rothenberg, J. Chem. Phys. **51**, 3389 (1969).
[23] S. Rothenberg, J. Am. Chem. Soc. **93**, 68 (1971).
[24] W. England, M. S. Gordon, and K. Ruedenberg, Theor. Chim. Acta **37**, 177 (1975).
[25] G. Náray-Szabó, G. Kramer, P. Nagy, and S. Kugler, J. Comput. Chem. **8**, 555 (1987).
[26] J. E. Carpenter and F. Weinhold, J. Am. Chem. Soc. **110**, 368 (1987).
[27] M. C. Krol and C. Altona, J. Mol. Phys. **72**, 375 (1991).
[28] J. D. Head and S. J. Silva, Int. J. Quantum Chem. **S26**, 229 (1992).
[29] J. L. Whitten, Chem. Phys. **177**, 387 (1993).
[30] P. G. Mezey, J. Math. Chem. **18**, 141 (1995).
[31] B. Kirtman, Int. J. Quantum Chem. **55**, 103 (1995).
[32] P. W. Anderson, Phys. Rev. **181**, 25 (1969).
[33] A. J. Skinner and D. G. Pettifor, J. Phys. Condens. Matter **3**, 2029 (1991).
[34] W. M. C. Foulkes, Phys. Rev. B **48**, 14 216 (1993).
[35] R. G. Woolley, Philos. Mag. B **69**, 745 (1994).
[36] J. Harris, Phys. Rev. B **31**, 1770 (1985).
[37] P. J. Feibelman, Phys. Rev. B **33**, 719 (1986).
[38] P. J. Feibelman, Phys. Rev. B **44**, 3916 (1991).
[39] M. P. Sears and P. A. Schultz (unpublished).
[40] G. Bachelet, D. Hamann, and M. Schlüter, Phys. Rev. B **26**, 4199 (1982).
[41] A. I. Kitaigorodsky, *Molecular Crystals and Molecules*, Physical Chemistry (Academic, New York, 1973), Vol. 29, and references therein.
[42] F. W. Averill and G. S. Painter, Phys. Rev. B **41**, 10 344 (1989).
[43] M. W. C. Foulkes and R. Haydock, Phys. Rev. B **39**, 12 520 (1989).
[44] K. Kobayashi, N. Kurita, H. Kumahora, and T. Kazutami, Phys. Rev. B **45**, 11 299 (1991).
[45] M. W. Finnis, J. Phys. Condens. Matter **2**, 331 (1990).
[46] N. Chetty, K. W. Jacobsen, and J. K. Nørskov, J. Phys. Condens. Matter **3**, 5437 (1991).
[47] A. J. Read and R. J. Needs, J. Phys. Condens. Matter **1**, 7565 (1989).
[48] H. J. M. Bowen *et al.*, *Tables of Interatomic Distances and Configuration in Molecules and Ions*, edited by A. D. Mitchell and L. C. Cross (The Chemical Society, London, 1958).
[49] T. L. Cottrell, *The Strengths of Chemical Bonds* (Butterworths, London, 1958).